Desalination and Water Treatment
www.deswater.com
doi: 10.5004/dwt.2018.22408

118 (2018) 249–257
June

Adsorption of low-level phosphate by Mg-Al layered double hydroxides and its competitive interaction with carbonate, sulfate, and chloride ion

Wei Liao, Hui-qiang Li*, Ping Yang

College of Architecture and Environment, Sichuan University, Chengdu 610065, China, Tel. +86 18980668020; email: lhq_scu@163.com (H.-q. Li), Tel. +86 18200288011; email: lw1993314@126.com (W. Liao), Tel. +86 18602804508; email: yping63@163.com (P. Yang)

Received 21 September 2017; Accepted 20 April 2018

ABSTRACT

Mg-Al-Cl and Mg-Al-NO_3 layered double hydroxides (LDHs) were synthesized by precipitation from homogeneous solution using urea hydrolysis. The scanning electron microscope images of the two LDHs showed plate-like particles. The Brunauer–Emmett–Teller surface area of the Mg-Al-Cl and Mg-Al-NO_3 LDHs were 21.37 and 38.45 m^2/g, respectively. The phosphate adsorption studies were carried out as a function of LDHs content, contact time, temperature, initial pH, and competitive anions. The Mg-Al-Cl and Mg-Al-NO_3 LDHs showed a good adsorption capacity on phosphate. It was found that the optimum condition for phosphate maximum removal rate onto LDHs were at pH of 4–10, temperature of 20°C and content of 0.05 g, the maximum removal rates of Mg-Al-Cl and Mg-Al-NO_3 LDHs for phosphate were more than 98%. The competitive anions (CO_3^{2-}, SO_4^{2-}, and Cl^-) had similar interferences on removal of phosphate by Mg-Al-Cl and Mg-Al-NO_3 LDHs, and the adverse impact of CO_3^{2-} was much greater than that of SO_4^{2-} and Cl^-. The X-ray diffraction patterns revealed the characteristic basal reflections of the LDHs materials. The Fourier transform infrared spectroscopy results confirmed the ion exchange and ligand exchange process during the adsorption of phosphate on the LDHs.

Keywords: Layered double hydroxides; Adsorption; Phosphate; Urea hydrolysis; Competitive anions

1. Introduction

Phosphorus is an essential nutrient and nonrenewable resource in aquatic ecosystems, which is widely used in industry, agriculture, and household applications [1]. However, the extensive use of phosphate inevitably causes elevated concentration in the receiving water bodies, which leads to algae bloom and degradation of water quality [2]. The first grade discharge limit of phosphate is 0.5 mg/L in China. Phosphate mostly exists as orthophosphates, polyphosphates, and organic phosphates in wastewater [3]. It is important to remove phosphate from aquatic system to eliminate eutrophication. There are many techniques to remove phosphate, such as ion-exchange [4], adsorption [5], chemical precipitation [6], and biological treatment [7]. Among them, adsorption has been regarded as a promising progress due to its flexibility, simplicity, ease of operation, less production of sludge, and low cost [8]. Various adsorbents, such as zeolite [9] and fly ash [10], have been studied for the removal of phosphate from aqueous solution. However, most of them are not selective and have low adsorption capacity. Yuan et al. [11] reported a significant phosphate removal rate by dolomite mineral, but the effluent phosphate concentration could not meet the discharge standards. Therefore, it is of great practical significance to seek for an adsorbent which can treat domestic sewage with low-level phosphate to reach the discharge standards.

Layered double hydroxides (LDHs) known as hydrotalcites are a kind of anionic clay, which have gained significant attention as effective adsorbent. LDHs are layered materials with a positive charged net, which are compensated by interlayer anions [12]. Because of the positive charge and exchangeable interlayer anion A^{n-}, LDHs possess exchange

* Corresponding author.

ability for organic and inorganic anions [13]. It is reported that LDHs can efficiently remove different anions, such as phosphate [14], nitrate [15], and humic acid [16] from aqueous solution. The crystal structure of LDHs varies with different M^{II}, M^{III}, x, A^{n-} and preparation method [17–19]. The influence of different metal precursors have been investigated by previous studies [20,21]. In most studies, LDHs were synthesized by conventional coprecipitation method. However, the method cannot control different parts of the slurry to maintain the same pH value, and it often causes strong agglomeration and low crystallinity [22]. The urea method uses urea as the precipitating agent. The urea hydrolysis process can provide a low degree of supersaturation during precipitation [22]. In this study, it is the first time that urea method was used to prepare LDHs, chloride and nitrate ion were chosen as interlayer anions to study the effect of phosphate adsorption.

Coexisting ions may compete with phosphate for the adsorption onto LDHs. The affinity sequence is NO_3^- < Cl^- < SO_4^{2-} < HPO_4^{2-} < CO_3^{2-} for LDHs [23]. Anions with high affinity are easily adsorbed onto LDHs. Competitive anions with high affinity on LDHs may have adverse impact on the phosphate adsorption. Das et al. [24] found competitive anions had detrimental effect on the percentage of adsorption. However, few studies have been reported on the effects of coexisting ions with different concentrations on phosphate adsorption using the LDHs. In order to investigate to what extent does different competitive anions impact on phosphate adsorption, it was shown for the first time that the impact of different concentrations coexisting anions on phosphate adsorption by Mg-Al-Cl LDHs and Mg-Al-NO_3 LDHs.

In this work, the effects of adsorbents content, initial pH and contact time on phosphate removal, and phosphate adsorption kinetics were investigated. Moreover, the interference effects of Cl^-, SO_4^{2-}, and CO_3^{2-} with different concentrations on phosphate adsorption onto LDHs were also investigated.

2. Materials and methods

2.1. Materials and chemicals

$MgCl_2{\cdot}6H_2O$, $Mg(NO_3)_2{\cdot}6H_2O$, $AlCl_3{\cdot}6H_2O$, $Al(NO_3)_2{\cdot}9H_2O$, KH_2PO_4, NaOH, Na_2CO_3, NaCl, Na_2SO_4, and urea used were AR grade. The aqueous phosphate solution used in this study was synthetic wastewater, and it was prepared by KH_2PO_4 in distilled water.

2.2. Synthesis

A mixture solution of $Mg(NO_3)_2{\cdot}6H_2O$, $Al(NO_3)_3{\cdot}9H_2O$, and urea (Mg^{2+} + Al^{3+} = 1 mol/L, Mg/Al = 3, urea/NO_3^- = 3) were added into a 500 mL three-neck flask and vigorously stirred at 100°C for 7 h. The slurry was subsequently aged at 90°C for 12 h. It was then centrifuged and washed thoroughly with distilled water till the washing was neutral. The precipitate was then dried overnight at 85°C.

The synthesis procedure of Mg-Al-Cl LDHs was similar to Mg-Al-NO_3 LDHs, but the metal salts were $MgCl_2{\cdot}6H_2O$ and $AlCl_3{\cdot}6H_2O$ instead of $Mg(NO_3)_2{\cdot}6H_2O$ and $Al(NO_3)_3{\cdot}9H_2O$.

2.3. Characterization

The images of synthesized Mg-Al LDHs were captured by a scanning electron microscope (SEM) (JSM-7500F, Japan). The specific surface areas and pore structures of the samples were detected by nitrogen adsorption based on Brunauer–Emmett–Teller (BET) and Barrett–Joyner–Halenda (BJH) methods using N_2 adsorption–desorption at 77 K on a surface area analyzer (ASAP2020, USA). Prior to BET measurement, the samples were degassed at 100°C for 4 h. The X-ray powder diffraction patterns of synthesized Mg-Al LDHs were carried out by a powder diffractometer using Cu Kα radiation at a scanning speed of 2°min^{-1} (PANalytical B.V., Holland). Fourier transform infrared spectroscopy (FTIR) spectrum of synthesized Mg-Al LDHs was obtained by FTIR spectrometer using KBr pellets over a range of 4,000–400 cm^{-1} (Nicolet 6700, USA). The metal ion concentrations were determined by inductively coupled plasma atomic emission spectroscopy (Jarrel-ASH, ICAP-9000) after phosphate adsorption by Mg-Al-Cl LDHs and Mg-Al-NO_3 LDHs at different pH.

2.4. Adsorption experiments

For the adsorption of phosphate, a stock solution (500 mg-P/L) was prepared from AR grade KH_2PO_4. The adsorption experiments were carried out in 250 mL conical flask by mixing 100 mL potassium dihydrogen phosphate solution at 5 mg-P/L with certain amount of LDHs under shaking. The mixtures were filtered at once after shaking to measure the residual phosphate concentration in the solution. The effects of initial pH, LDHs content, contact time, and temperature on phosphate adsorption were studied. The initial pH of the solution was adjusted by addition of 0.1 mol/L HCl or NaOH solution and the supernatant pH was measured after adsorption. The volume of the HCl or NaOH added for pH adjustment never exceeded 1% of total volume. The residual concentration of phosphate was determined by molybdate blue spectrophotometric method. Each experiment was made induplicate. The adsorption capacity q_e (mg/g) and removal rate R (%) were calculated as the following Eqs. (1) and (2):

$$q_e = \frac{(C_1 - C_e)\cdot V}{W} \tag{1}$$

$$R(\%) = \frac{C_0 - C_e}{C_0} \times 100\% \tag{2}$$

where C_0 is the initial concentration of the P (mg-P/L), C_e is the equilibrium or residual P concentration (mg-P/L), V is the volume of the solution (L), and W is the mass of adsorbent (g).

2.5. Adsorption kinetics

The pseudo-first-order and pseudo-second-order kinetics were used to analyze adsorption kinetic data. The linear form of the pseudo-first-order (Eq. (3)) and the pseudo-second-order (Eq. (4)) equations could be expressed as follows [25]:

$$\ln(q_e - q_t) = \ln q_e - k_1 t \tag{3}$$

$$\frac{t}{q_t} = \frac{1}{k_2 q_e^2} + \frac{t}{q_e} \quad (4)$$

where q_e and q_t (mg/g) are the amounts of phosphate adsorbed at equilibrium and at time t (min), respectively. k_1 (min^{-1}) is the rate constant of the pseudo-first-order model and k_2 is the rate constant of the pseudo-second-order model (g/(mg min)).

3. Results and discussion

3.1. Characteristics of the LDHs

The SEM images were recorded to investigate the morphology of the synthesized LDHs. It can be seen from Fig. 1, both of the LDHs showed a well-developed layered with fine dispersion of the plate-like particles. The LDHs consist of aggregates of primary sheet, and their surfaces were smooth. The surface of Mg-Al-NO_3 LDHs was more homogeneous.

Nitrogen adsorption isotherm and corresponding pore size distribution (PSD) of the LDHs are shown in Fig. 2 and the porous structure parameters are compiled in Table 1. The PSD of both samples were calculated with BJH method using the boundaries p/p_0 between 0.05 and 0.35 in the desorption data of the isotherms. According to the classification of IUPAC, the adsorption and desorption branches of the LDHs can be classified as type III-like adsorption isotherms with a H3-type hysteresis loop for the desorption isotherms, which is observed with aggregates of plate-like particles giving rise to slit-shaped pores [26]. The average pore diameters of Mg-Al-Cl LDHs and Mg-Al-NO_3 LDHs showed mesopore size (2–50 nm) dominated in the adsorbents. The BET total surface area of Mg-Al-Cl LDHs (21.37 m^2/g) was larger than that of Mg-Al-NO_3 LDHs (38.45 m^2/g). For adsorbents, a large surface area can provide more adsorption sites.

The X-ray diffraction (XRD) patterns corresponding to the synthesized LDHs are illustrated in Fig. 3. The patterns of

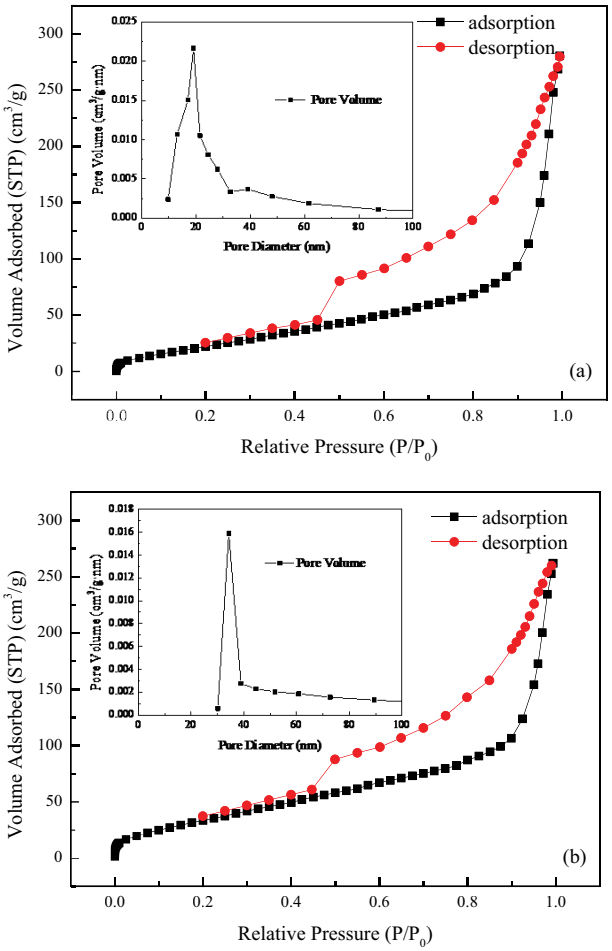

Fig. 2. Isotherm curve of N_2 adsorption–desorption and pore size distribution of (a) Mg-Al-Cl LDHs and (b) Mg-Al-NO_3 LDHs.

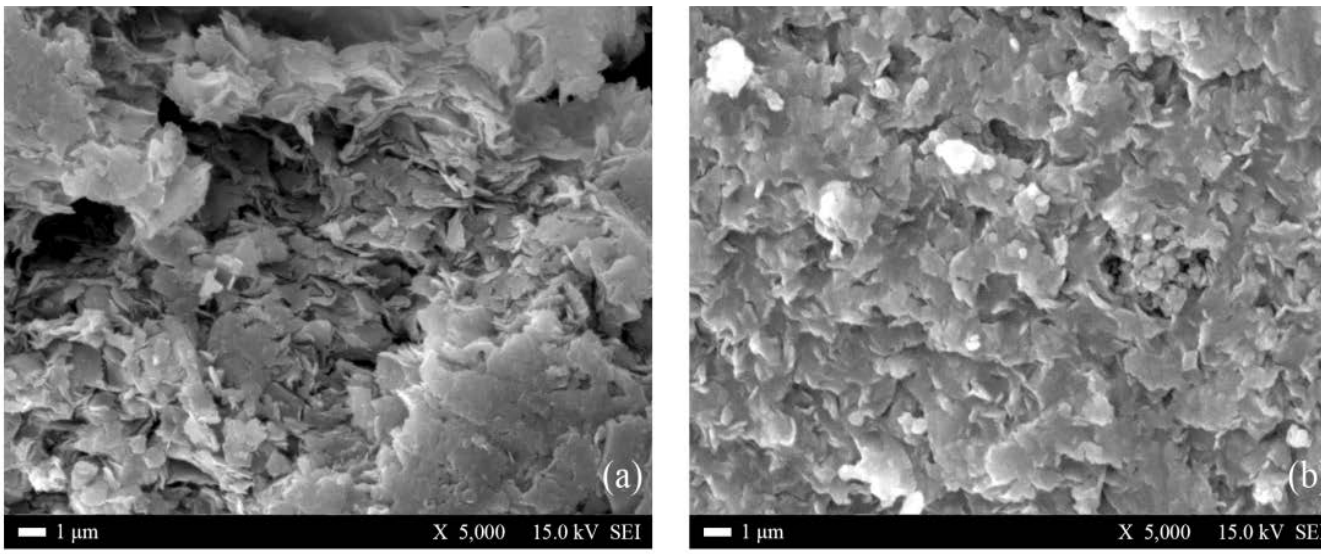

Fig. 1. SEM of (a) Mg-Al-Cl LDHs and (b) Mg-Al-NO_3 LDHs.

Table 1
Porous structure parameters of the LDHs

Adsorbents	Surface area (S_{BET}) (m^2/g)	Pore volume (cm^3/g)	Average pore diameter (nm)
Mg-Al-Cl LDHs	21.37	0.26	23.74
Mg-Al-NO_3 LDHs	38.45	0.17	34.62

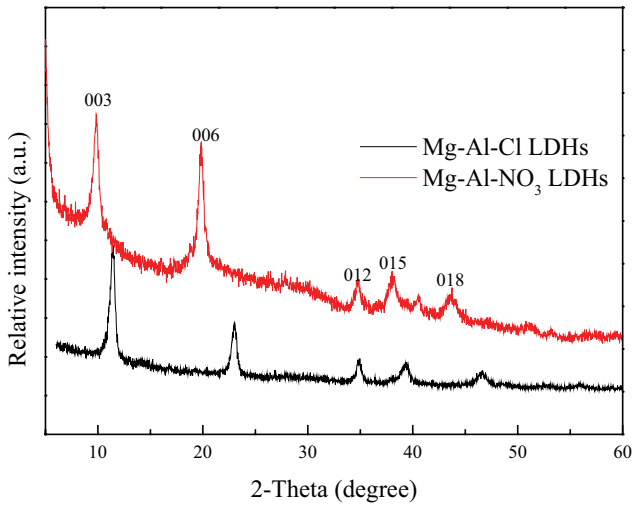

Fig. 3. XRD patterns of LDHs.

Mg-Al-Cl LDHs and Mg-Al-NO_3 LDHs were similar to each other and all diffraction peaks can be attributed to a typical crystal structure of the LDHs. The sharp and symmetric peaks for (003) and (006) planes and broad peaks assigned to (012), (015), and (018) planes were indexed to a hexagonal LDHs lattice with rhombohedral 3R symmetry [26,27]. Diffraction peaks owing to impurities were not observed. The characteristics reflection bands of the two materials showed sharp and symmetric peaks at lower 2θ values which indicated a good crystallinity grade using urea method.

The interlayer *d*-spacing d_{003} and d_{006} of Mg-Al-Cl LDHs were found to be 7.8 and 3.8 nm, which were 8.9 and 4.5 nm for the Mg-Al-NO_3 LDHs. The d_{003} was twice as much as d_{006}, indicating a favorable layer structure. The *d*-spacing is related to the size of interlayer anions [28]. The *d*-spacing of Mg-Al-Cl LDHs was smaller than Mg-Al-NO_3 LDHs, which was due to the radius of Cl^- is smaller than that of NO_3^-.

3.2. Effect of operation parameters on adsorption performance

3.2.1. Content of the LDHs

The addition of Mg-Al-Cl and Mg-Al-NO_3 LDHs content significantly influenced on the phosphate adsorption. Variation of adsorbent content on phosphate removal is shown in Fig. 4. The removal rate of phosphate was improved with the amount of LDHs increasing from 0.01 to 0.05 g in 100 mL phosphate solution.

With the enhancement of LDHs content, the amount of adsorption sites was increased. The removal rate of phosphate was more than 98% for both Mg-Al-Cl and Mg-Al-NO_3 LDHs at content of 0.05 g. However, after content of 0.05 g,

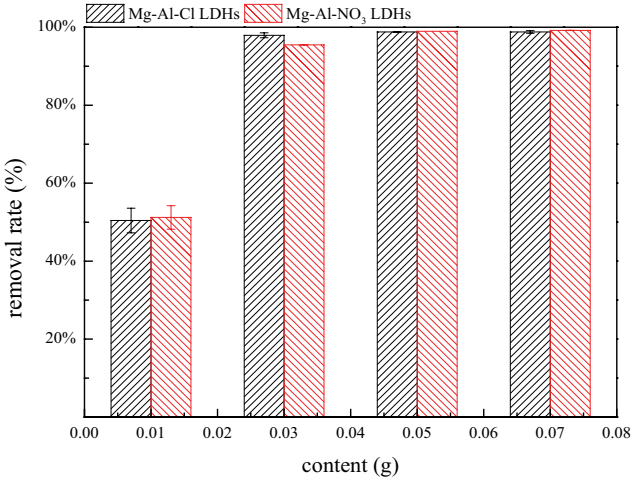

Fig. 4. Effect of LDHs content on phosphate removal.

an equilibrium adsorption was obtained. There was no significant change in removal rate of phosphate with the content increased to 0.07 g. The result would be caused by the overlapping of active sites at higher content as observed in previous study as well [29]. At low adsorbent content, all kinds of surface sites were entirely exposed for adsorption. But at higher adsorbent content, collision between solid particles probably created particle aggregation, then causing a decrease in the total surface area and active sites [30]. The high masses represented a waste of adsorbent. So, 0.05 g was considered as optimum content and was used for subsequent study.

3.2.2. Contact time

The adsorption as a function of contact time was conducted at 20°C and the initial phosphate concentration was 5 mg-P/L. As Fig. 5 indicates, the removal rate of phosphate was rapidly increased in the first 30 min and reached equilibrium at about 45 min. With contact time increasing from 5 to 45 min, the removal rate of phosphate was improved from 92.6% to 98.8% for the Mg-Al-Cl LDHs and from 66.4% to 99.1% for the Mg-Al-NO_3 LDHs. Yu et al. [31] reported Zn_2Al-PMA-LDHs took approximately 4 h to reach phosphate adsorption equilibrium at 293 and 303 K. By contrast, the urea synthesized Mg-Al LDHs reached equilibrium quicker so as to save much time in practical application. In the first 30 min, the phosphate removal of the Mg-Al-Cl LDHs was much higher than the Mg-Al-NO_3 LDHs. While the equilibrium adsorption rate of the Mg-Al-Cl LDHs was 98.8%, which was slightly lower than that of Mg-Al-NO_3 LDHs (99.1%). The adsorption progress was fast in the first 30 min may attribute to the sufficient adsorption sites and the high solute concentration gradient. At the beginning, higher phosphate concentration provided higher driving force for the anion from the solution to the LDHs, which led higher velocity of phosphate removal. The adsorption sites and the solute concentration gradient would decline with the proceeding of adsorption, which induced the decrease of adsorption rate. Both of the adsorptions reached equilibrium

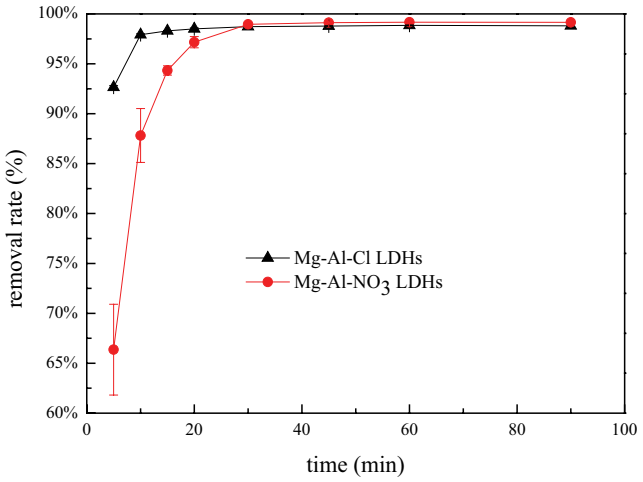

Fig. 5. Effect of contact time on phosphate removal.

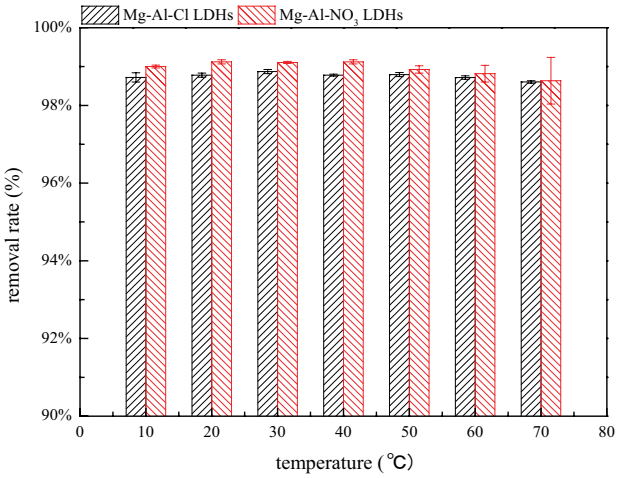

Fig. 6. Effect of temperature on phosphate removal.

at 45 min. Therefore, in the following experiments, the contact time was set as 45 min.

In order to clarify the adsorption kinetics of phosphate onto LDHs, the pseudo-first-order and pseudo-second-order kinetics models were used. The first-order and second-order equations describe the kinetics of the solid–solution system based on mononuclear and binuclear adsorption [32]. For fitting of pseudo-first-order and pseudo-second-order models, all the data points were used. The fitting curves for pseudo-first-order and pseudo-second-order models were presented in Fig. S1 and the kinetic parameters and correlation coefficients (R^2) are listed in Table 2. The greater kinetic rate constant value of Mg-Al-Cl LDHs indicated higher velocity of phosphate removal than that of Mg-Al-NO_3 LDHs. The results were in agreement with the experiment results. The greater correlation coefficient values were obtained in the pseudo-first-order model comparing with pseudo-second-order, and the theoretical uptakes q_e (cal) were in better agreement with the experimental uptakes q_e (exp) for the pseudo-first-order model. So, it concluded that phosphate adsorption on the LDHs was better fitted to the pseudo-first-order model. Similar results have been reported for the adsorption of phosphate on Mg-Al LDHs [24].

3.2.3. Temperature

Effect of temperature on the adsorption of phosphate by LDHs was studied. The results are shown in Fig. 6. Temperature had a very small influence on the adsorption for both adsorptions. There was no distinct variation trend when the temperature changed between 10°C and 40°C. The removal rates of phosphate were 98.8% and 99.1% for Mg-Al-Cl LDHs and Mg-Al-NO_3 LDHs, respectively. The removal rates were higher than that of activated carbon residue [33]. With the temperature further increasing from 40°C to 70°C, the removal rate of phosphate slightly decreased to 98.6% for both Mg-Al-Cl LDHs and Mg-Al-NO_3 LDHs, respectively. So, the influence of temperature on the adsorption of phosphate for the Mg-Al-Cl LDHs and Mg-Al-NO_3 LDHs was negligible. Moreover, the LDHs showed a good stability under high temperature condition.

3.2.4. pH

The pH value is one of the most important parameters in adsorption experiments. The effect of different initial pH values ranging from 2 to 12 on the adsorption of phosphate was studied. The results are represented in Fig. 7(a). It was clear that the phosphate removal rate of Mg-Al-Cl LDHs (~98%) and Mg-Al-NO_3 LDHs (~99%) was steady when pH value was in the range of 4–10. It came to a conclusion that LDHs had a good adsorption capacity in a wide range of initial pH value. Under strongly acidic (pH = 2) or alkaline (pH = 12) condition, the inhibitory effect on phosphate removal was obvious, and the impact on the performance of the Mg-Al-NO_3 LDHs was much greater than on the Mg-Al-Cl LDHs. LDHs are alkaline materials, and the adsorption capacity would be greatly reduced because of layer structure destroyed by strong acid. Under strongly alkaline condition, OH^- would compete with phosphate and influence the adsorption performance. The dissolution properties of Mg-Al-Cl LDHs and

Table 2
Kinetic parameters and correlation coefficients (R^2)

Adsorbent	q_e, exp (mg/g)	Pseudo-first order			Pseudo-second order		
		q_e, cal (mg/g)	k_1 (min^{-1})	R^2	q_e, cal (mg/g)	k_2 (g/mg min)	R^2
Mg-Al-Cl LDHs	10.47	10.45	0.5595	0.9872	10.58	0.2821	0.8578
Mg-Al-NO_3 LDHs	9.91	9.89	0.2200	0.9981	10.53	0.0396	0.9062

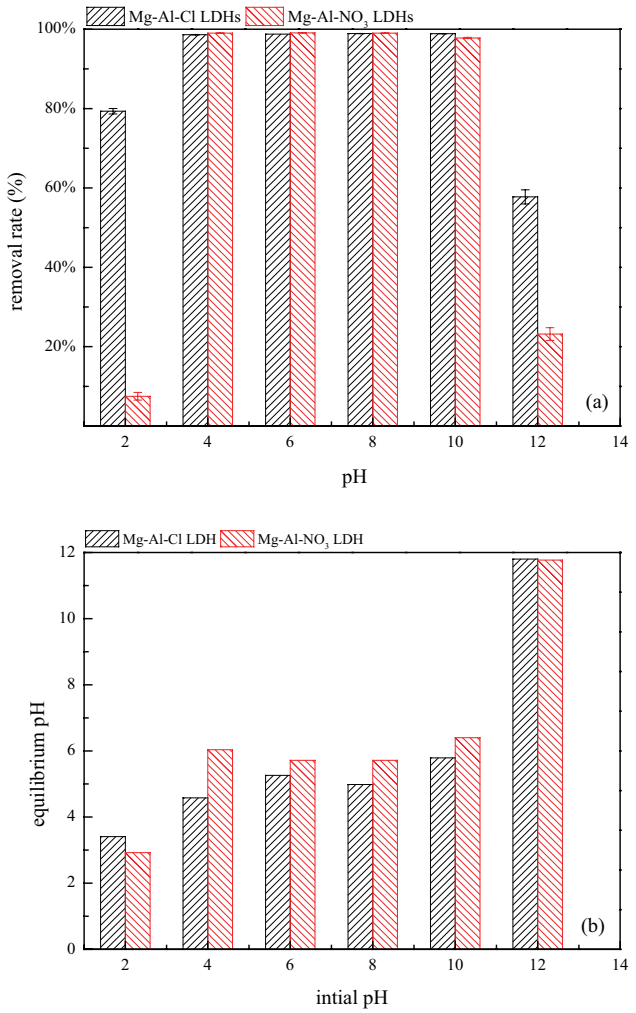

Fig. 7. (a) Effect of pH on phosphate removal and (b) the equilibrium pH after adsorption.

Mg-Al-NO_3 LDHs under different pH were detected and the results are compiled in Table S1. Under strong acid condition, the structures of Mg-Al-Cl LDHs and Mg-Al-NO_3 LDHs were destroyed due to the serious dissolution effect of Mg and Al. From this result, it can be concluded that the structure of Mg-Al-NO_3 LDHs was more easily destroyed under extreme condition. For Mg-Al-Cl LDHs, the structure was relatively stable. The phosphate removal rate was nearly 80% when pH decreased to 2. The metal ions content in the solution were decreased under weak-acidic and alkaline condition, indicating the dissolution effect was weaken and the structures could keep stable. At pH of 12, Mg content was not detected because of the released Mg^{2+} react with phosphate to form precipitate. So, phosphate was mainly adsorbed onto Mg-Al-Cl LDHs and Mg-Al-NO3 LDHs through ion exchange with the interlayer anions. Under alkaline condition, the removal of phosphate was partially contributed by dissolved Mg ions to form precipitate.

Mg-Al-Cl LDHs can be applied to treat acidic sewage without adjustment of pH value. The pH values of wastewater fluctuate widely. After adsorption by LDHs the pH would be adjusted to a certain range due to the buffering capacity. This was beneficial to subsequent treatment. Therefore, the pH values after the equilibrium of the adsorption are shown in Fig. 7(b). The results revealed that the LDHs had a strong buffering capacity, because the final pH remained from 4 to 6 for an initial pH range of 4–10. The buffering capacity of Ca-based LDHs was also reported [21].

3.3. Effect of competitive anions

Common anions, such as CO_3^{2-}, SO_4^{2-}, and Cl^-, are generally presented in phosphate containing wastewater. The anions may compete with phosphate for adsorption onto LDHs. The effect of competitive anions was studied using solutions containing 5 mg-P/L phosphate and different concentration gradients of the competitive anions. The lowest concentrations of anions were up to the concentration have negligible impact on phosphate adsorption. The highest concentrations of anions were up to the concentration could make the removal rate of phosphate below 50%. The studies for competitive anions were conducted without adjusting the pH of the solution. The initial pH of the experiments for competitive anions was about 6–7. The results are presented in Fig. 8. The performance of Mg-Al-Cl LDHs and Mg-Al-NO_3 LDHs on phosphate removal showed a similar trend interrupted by CO_3^{2-}, SO_4^{2-}, and Cl^-, but the inhibitory effect on Mg-Al-Cl LDHs was stronger.

With the increase of coexisting anion concentration, the phosphate removal efficiency of the two LDHs decreased. The influence of carbonate ions on the adsorption was the largest. When the concentration of carbonate ions added to 100 mg/L, the removal rate dropped to 18.6% for the Mg-Al-Cl LDHs and 17.1% for the Mg-Al-NO_3 LDHs. Only when the concentration of carbonate ions was lower than 1 mg/L the inhibitory effect of carbonate could be neglected. Chloride ions had minimal adverse effect on the phosphate adsorption. 1,000 mg/L of chloride almost had no influence on the adsorption efficiency of the LDHs. With the concentration of chloride increasing to 50 g/L, the removal rate decreased to 58.8% for the Mg-Al-Cl LDHs and 60.1% for the Mg-Al-NO_3 LDHs. Similar conclusions were also achieved by other studies on the influence of coexisting anions [32,34]. The results in this study confirmed the anion affinity toward LDHs follow the trend: $CO_3^{2-} > SO_4^{2-} > Cl^-$. The LDHs have more affinity toward divalent anions compared with monovalent anions, and the anions with a higher charge density have a more intense interfering effect.

To elucidate the interaction mechanisms between phosphate and LDHs, FTIR analyses and XRD pattern changes of Mg-Al-Cl LDHs and Mg-Al-NO_3 LDHs before and after adsorption with the disturbance of competitive anions (100 mg/L CO_3^{2-}; 5,000 mg/L SO_4^{2-}; 50 g/L Cl^-) were conducted. FTIR spectra are shown in Fig. 9. Broad and intense absorption bands around 3,500 cm^{-1} (O–H stretching vibration) and about at 1,700–1,610 cm^{-1} (O–H bending vibration) indicated the presence of interstitial water molecules [23]. Absorption band at 664 cm^{-1} ($\sigma_{O\text{-}M}$) and at 446 cm^{-1} ($\sigma_{O\text{-}M\text{-}O}$) is characteristic of lattice vibrations of [Mg,Al] octahedral sheets which evidences the crystallization of the LDHs phase [35]. The bands around 1,384 cm^{-1} (Fig. 9(b)) were observed, implying the large amount of NO_3^- species intercalated in the interlayer

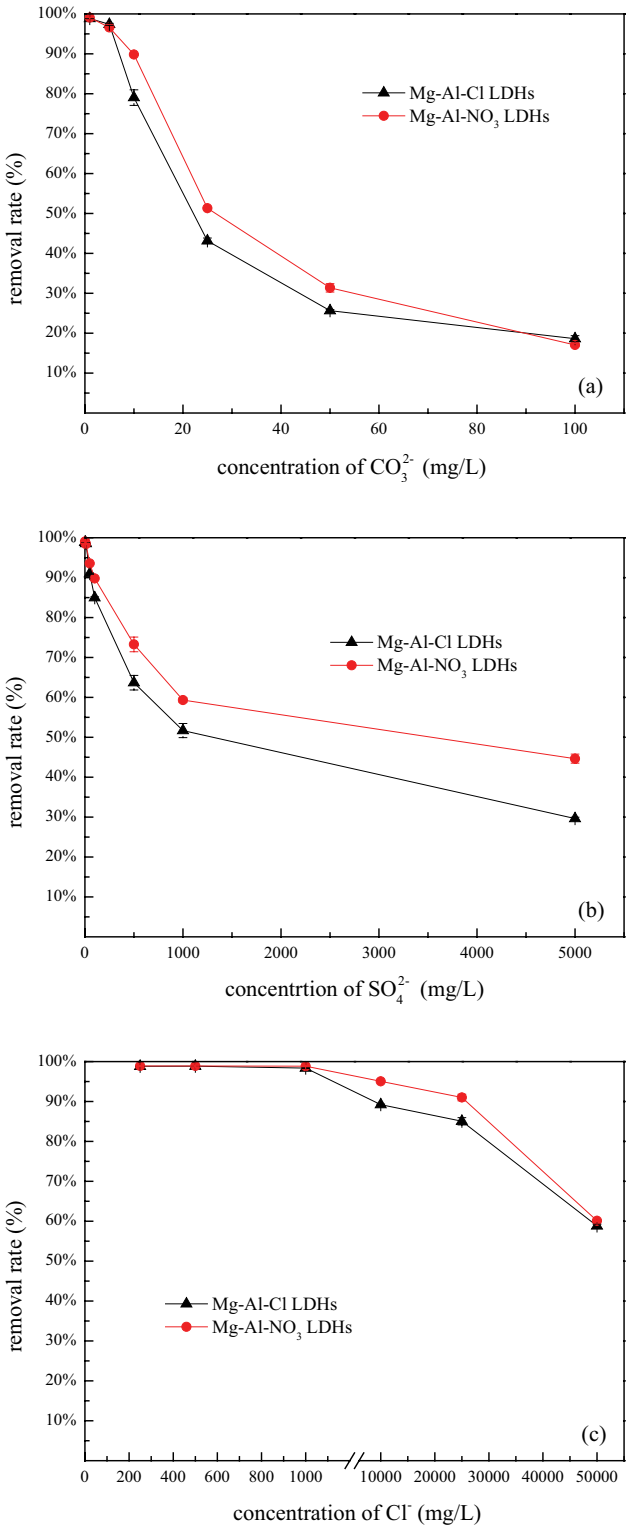

Fig. 8. Effect of competitive anions with different concentrations on phosphate removal. (a) carbonate, (b) sulfate, and (c) chloride.

space of Mg-Al-NO_3 LDHs [23]. After intercalation with the phosphate solution, a new band characteristic of phosphate ion appeared at 1,066 cm^{-1} (Fig. 9(a)) and 1,056 cm^{-1} (Fig. 9(b)) that validated the adsorption of phosphate on LDHs through

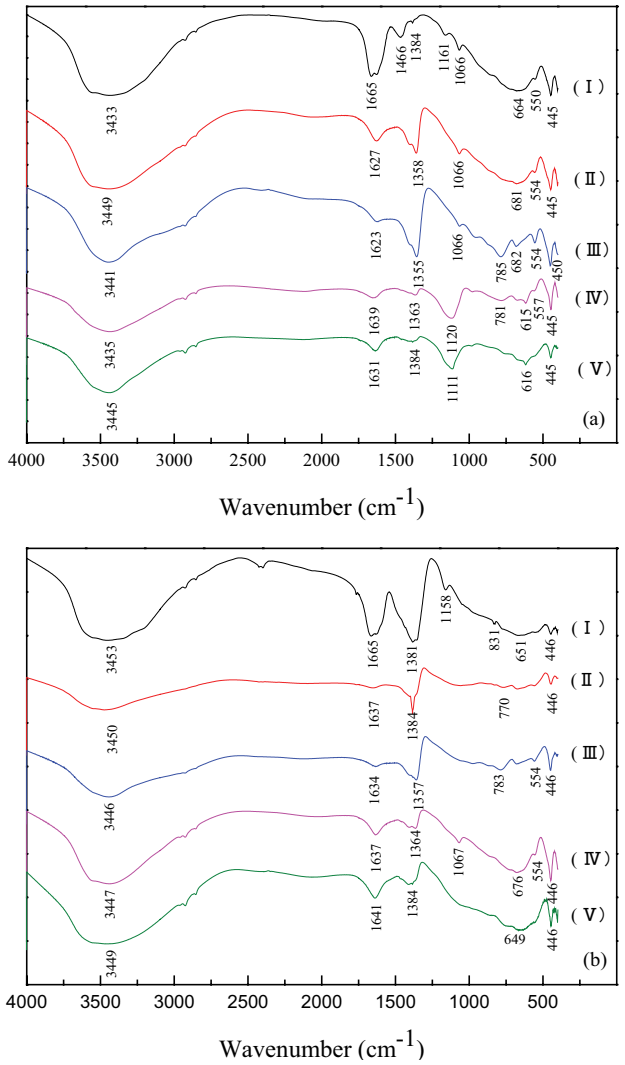

Fig. 9. FTIR of (a) Mg-Al-Cl LDHs and (b) Mg-Al-NO_3LDHs ((I): LDH; (II): phosphate; (III): phosphate + carbonate; (IV): phosphate + sulfate; (V): phosphate + chloride).

ion exchange [32]. From the presence of new peak, it could be deduced that the surface hydroxyl group (M-OH) of LDHs was exchanged by the adsorbed phosphate (M-O-P), indicating a ligand exchange process occurred during adsorption [14].

With the addition of competitive anions, interlayer ions were partly replaced by carbonate ions [ν (CO_3^{2-}): 1,357 cm^{-1} (Fig. 9(b))] [36] and sulfate ions [ν (SO_4^{2-}): 1,120 cm^{-1} (Fig. 9(a))] [23]. It can be speculated that the adsorption on Mg-Al-Cl and Mg-Al-NO_3 LDHs mainly via ion exchange. The FTIR spectra did not show such a strong band for phosphate in Fig. 9(b), which may due to less phosphate was adsorbed onto Mg-Al-NO_3 LDHs in competitive ion solution. The results indicated greater affinity of the synthesized LDHs toward carbonate and sulfate than phosphate. The FTIR spectra confirmed ion exchange and ligand progress during the adsorption.

The XRD patterns after phosphate adsorption in single and binary system are shown in Fig. 10. Those patterns presented a similar pattern as the original precursor, and

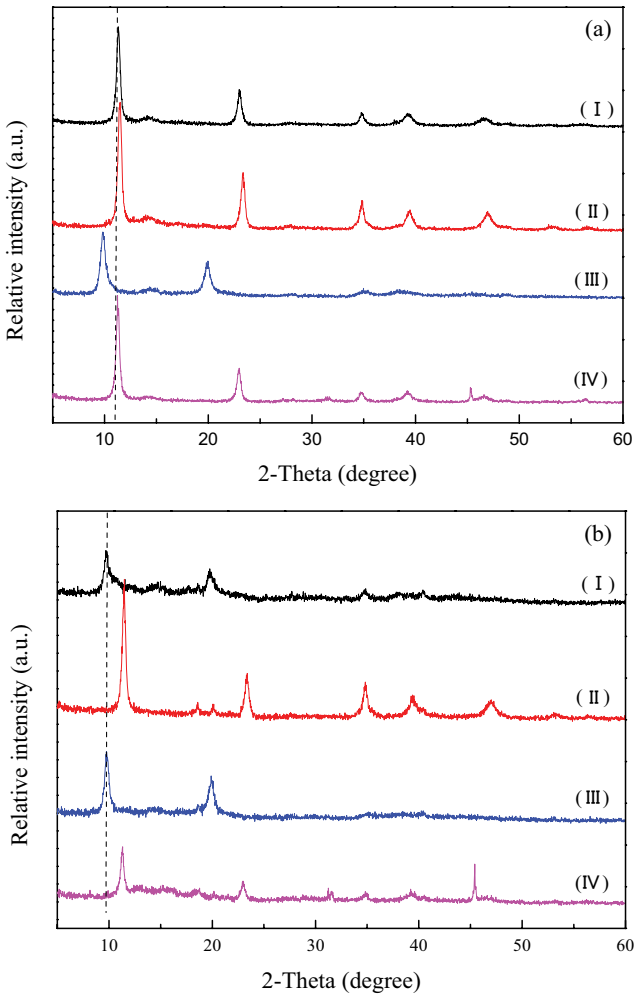

Fig. 10. XRD patterns of (a) Mg-Al-Cl LDHs and (b) Mg-Al-NO_3 LDHs ((I): phosphate; (II): phosphate + carbonate; (III): phosphate + sulfate; (IV): phosphate + chloride).

the layered structure was retained in all cases. However, the *d*-spacing d_{003} changed to different degree after adsorption of phosphate and other competition anions. This result indicated that the adsorbed anions were intercalated into the interlayer, the layered structure retained after the adsorption, but the interlayer spacing changed. From XRD and FTIR analyses, it can conclude that anions adsorption onto Mg-Al-Cl LDHs and Mg-Al-NO_3 LDHs via ion exchange.

4. Conclusion

In this study, both Mg-Al-Cl LDHs and Mg-Al-NO_3 LDHs showed significant adsorption abilities for phosphate. The removal of phosphate depended on the process parameters. The adsorption of phosphate onto Mg-Al-Cl and Mg-Al-NO_3 LDHs reached completely equilibrium within 45 min. Phosphate adsorption on Mg-Al-Cl and Mg-Al-NO_3 LDHs were better fitted to pseudo-first-order kinetic model. The pH had a detrimental influence on phosphate adsorption under strong acidic and alkali condition. The structure of Mg-Al-Cl LDHs was steadier than Mg-Al-NO_3 LDHs. At pH range of 4–10, the maximum removal rates of Mg-Al-Cl and Mg-Al-NO_3 LDHs for phosphate were more than 98%. The results were superior to activated carbon residue. The effects of coexisting anions on the phosphate adsorption capacity declined with the following order: $CO_3^{2-} > SO_4^{2-} > Cl^-$, and the inhibitory influence increased with the elevating of the concentration of coexisting anions. The results of FTIR spectra and XRD indicated that ion exchange and ligand exchange were mainly responsible for phosphate adsorption by Mg-Al-Cl LDHs and Mg-Al-NO_3 LDHs. The results derived from this study suggested that the Mg-Al-Cl LDHs and Mg-Al-NO_3 LDHs are promising adsorbents for the removal of phosphate in aqueous solution.

Acknowledgment

This research was supported by the National Natural Science Foundation of China (no. 51308362).

References

[1] Q. Zhou, X. Wang, J. Liu, L. Zhang, Phosphorus removal from wastewater using nano-particulates of hydrated ferric oxide doped activated carbon fiber prepared by sol–gel method, Chem. Eng. J., 200–202 (2012) 619–626.
[2] A. Mikhak, A. Sohrabi, M.Z. Kassaee, M. Feizian, M. Najafi Disfani, Removal of nitrate and phosphate from water by clinoptilolite-supported iron hydroxide nanoparticle, Arabian J. Sci. Eng., 42 (2017) 2433–2439.
[3] N. Baliarsingh, K.M. Parida, G.C. Pradhan, Influence of the nature and concentration of precursor metal ions in the brucite layer of LDHs for phosphate adsorption – a review, RSC Adv., 3 (2013) 23865–23878.
[4] W. Mo, M. Zhang, C. Kang, Y. Lun, C. Chen, M. Meng, M. Chen, Preparation of a new ion-exchange resin from cassava stalk for effective removal of phosphate ions from wastewater, Fresenius Environ. Bull., 24 (2006) 740–747.
[5] X. Liu, L. Zhang, Removal of phosphate anions using the modified chitosan beads: adsorption kinetic, isotherm and mechanism studies, Powder Technol., 277 (2015) 112–119.
[6] H. Huang, J. Liu, P. Zhang, D. Zhang, F. Gao, Investigation on the simultaneous removal of fluoride, ammonia nitrogen and phosphate from semiconductor wastewater using chemical precipitation, Chem. Eng. J., 307 (2017) 696–706.
[7] D. Mulkerrins, C. Jordan, S. Mcmahon, E. Colleran, Evaluation of the parameters affecting nitrogen and phosphorus removal in anaerobic/anoxic/oxic (A/A/O) biological nutrient removal systems, J. Chem. Technol. Biotechnol., 75 (2015) 261–268.
[8] C. Xiang, X. Huang, X. Wang, D. Sun, Influence of calcination on the adsorptive removal of phosphate by Zn-Al layered double hydroxides from excess sludge liquor, J. Hazard. Mater., 177 (2010) 516.
[9] T. Liu, B. Chang, K. Wu, The performance of phosphate removal using aluminium-manganese bimetal oxide coated zeolite: batch and dynamic adsorption studies, Desal. Wat. Treat., 57 (2016) 4220–4233.
[10] R.E. Masto, R. Verma, L.C. Ram, V.A. Selvi, J. George, A.K. Sinha, Phosphorus removal using lignite fly ash, Energy Sources Part A, 37 (2015) 735–741.
[11] X. Yuan, W. Xia, J. An, J. Yin, X. Zhou, W. Yang, Kinetic and thermodynamic studies on the phosphate adsorption removal by dolomite mineral, J. Chem., 2015 (2015) 1–8.
[12] M. Zubair, M. Daud, G. McKay, F. Shehzad, M.A. Al-Harthi, Recent progress in layered double hydroxides (LDH)-containing hybrids as adsorbents for water remediation, Appl. Clay Sci., 143 (2017) 279–292.
[13] A. Halajnia, S. Oustan, N. Najafi, A.R. Khataee, A. Lakzian, The adsorption characteristics of nitrate on Mg–Fe and Mg–Al layered double hydroxides in a simulated soil solution, Appl. Clay Sci., 70 (2012) 28–36.

[14] K. Yang, L.G. Yan, Y.M. Yang, S.J. Yu, R.R. Shan, H.Q. Yu, B.C. Zhu, B. Du, Adsorptive removal of phosphate by Mg–Al and Zn–Al layered double hydroxides: kinetics, isotherms and mechanisms, Sep. Purif. Technol., 124 (2014) 36–42.
[15] R. Sasai, W. Norimatsu, Y. Matsumoto, Nitrate-ion-selective exchange ability of layered double hydroxide consisting of MgII and FeIII, J. Hazard. Mater., 215–216 (2012) 311–314.
[16] G. Zhang, T. Wu, Y. Li, X. Huang, Y. Wang, G. Wang, Sorption of humic acid to organo layered double hydroxides in aqueous solution, Chem. Eng. J., 191 (2012) 306–313.
[17] Y. Wang, H. Gao, Compositional and structural control on anion sorption capability of layered double hydroxides (LDHs), J. Colloid Interface Sci., 301 (2006) 19–26.
[18] H. He, H. Kang, S. Ma, Y. Bai, X. Yang, High adsorption selectivity of ZnAl layered double hydroxides and the calcined materials toward phosphate, J. Colloid Interface Sci., 343 (2010) 225–231.
[19] J. Wang, X. Wang, L. Tan, Y. Chen, T. Hayat, J. Hu, A. Alsaedi, B. Ahmad, W. Guo, X. Wang, Performances and mechanisms of Mg/Al and Ca/Al layered double hydroxides for graphene oxide removal from aqueous solution, Chem. Eng. J., 297 (2016) 106–115.
[20] S. Tezuka, R. Chitrakar, K. Sakane, A. Sonoda, K. Ooi, T. Tomida, The synthesis and phosphate adsorptive properties of Mg(II)–Mn(III) layered double hydroxides and their heat-treated materials, Bull. Chem. Soc. Jpn., 77 (2004) 2101–2107.
[21] S.M. Ashekuzzaman, J.-Q. Jiang, Study on the sorption–desorption–regeneration performance of Ca-, Mg- and CaMg-based layered double hydroxides for removing phosphate from water, Chem. Eng. J., 246 (2014) 97–105.
[22] J. Liu, J. Song, H. Xiao, L. Zhang, Y. Qin, D. Liu, W. Hou, N. Du, Synthesis and thermal properties of ZnAl layered double hydroxide by urea hydrolysis, Powder Technol., 253 (2014) 41–45.
[23] A. Halajnia, S. Oustan, N. Najafi, A.R. Khataee, A. Lakzian, Adsorption–desorption characteristics of nitrate, phosphate and sulfate on Mg–Al layered double hydroxide, Appl. Clay Sci., 80–81 (2013) 305–312.
[24] J. Das, B.S. Patra, N. Baliarsingh, K.M. Parida, Adsorption of phosphate by layered double hydroxides in aqueous solutions, Appl. Clay Sci., 32 (2006) 252–260.
[25] W. Yao, S. Yu, J. Wang, Y. Zou, S. Lu, Y. Ai, N.S. Alharbi, A. Alsaedi, T. Hayat, X. Wang, Enhanced removal of methyl orange on calcined glycerol-modified nanocrystallined Mg/Al layered double hydroxides, Chem. Eng. J., 307 (2017) 476–486.
[26] R.M.M. Santos, J. Tronto, V. Briois, C.V. Santilli, Thermal decomposition and recovery properties of ZnAl–CO_3 layered double hydroxide for anionic dye adsorption: insight into the aggregative nucleation and growth mechanism of the LDH memory effect, J. Mater. Chem. A, 5 (2017) 9998–10009.
[27] V. Gbb, O.A. Oyetade, S. Rana, B.S. Martincigh, S.B. Jonnalagadda, V.O. Nyamori, Facile synthesis of three-dimensional Mg-Al layered double hydroxide/partially reduced graphene oxide nanocomposites for the effective removal of Pb(2+) from aqueous solution, ACS Appl. Mater. Interfaces, 9 (2017) 17290.
[28] G.V. Manohara, S.V. Prasanna, P.V. Kamath, Structure and composition of the layered double hydroxides of Mg and Fe: implications for anion-exchange reactions, Eur. J. Inorg. Chem., 2011 (2011) 2624–2630.
[29] M. Islam, R. Patel, Synthesis and physicochemical characterization of Zn/Al chloride layered double hydroxide and evaluation of its nitrate removal efficiency, Desalination, 256 (2010) 120–128.
[30] S. Yanming, L. Dongbin, L. Shifeng, F. Lihui, C. Shuai, M.A. Haque, Removal of lead from aqueous solution on glutamate intercalated layered double hydroxide, Arabian J. Chem., 10 (2017) S2295–S2301.
[31] Q. Yu, Y. Zheng, Y. Wang, S. Liang, H. Wang, Y. Zheng, H. Ning, Q. Li, Highly selective adsorption of phosphate by pyromellitic acid intercalated ZnAl-LDHs: assembling hydrogen bond acceptor sites, Chem. Eng. J., 260 (2015) 809–817.
[32] C. Novillo, D. Guaya, A.P. Avendaño, C. Armijos, J.L. Cortina, I. Cota, Evaluation of phosphate removal capacity of Mg/Al layered double hydroxides from aqueous solutions, Fuel, 138 (2014) 72–79.
[33] S. Kilpimaa, H. Runtti, T. Kangas, U. Lassi, T. Kuokkanen, Physical activation of carbon residue from biomass gasification: novel sorbent for the removal of phosphates and nitrates from aqueous solution, J. Ind. Eng. Chem., 21 (2015) 1354–1364.
[34] D. Wan, H. Liu, R. Liu, J. Qu, S. Li, J. Zhang, Adsorption of nitrate and nitrite from aqueous solution onto calcined (Mg–Al) hydrotalcite of different Mg/Al ratio, Chem. Eng. J., 195–196 (2012) 241–247.
[35] M. Adachi-Pagano, C. Forano, J.-P. Besse, Synthesis of Al-rich hydrotalcite-like compounds by using the urea hydrolysis reaction — control of size and morphology, J. Mater. Chem., 13 (2003) 1988–1993.
[36] M. Zhang, B. Gao, Y. Yao, M. Inyang, Phosphate removal ability of biochar/MgAl-LDH ultra-fine composites prepared by liquid-phase deposition, Chemosphere, 92 (2013) 1042–1047.

Supplementary

Table S1
The dissolution properties of Mg-Al-Cl LDHs and Mg-Al-NO_3 LDHs

pH	Mg-Al-Cl LDHs		Mg-Al-NO_3 LDHs	
	Mg (mg/L)	Al (mg/L)	Mg (mg/L)	Al (mg/L)
2	34.2	30.4	57.2	53.3
6	6.18	0.28	6.49	0.07
12	ND	2.38	ND	3.35

ND: not detected.

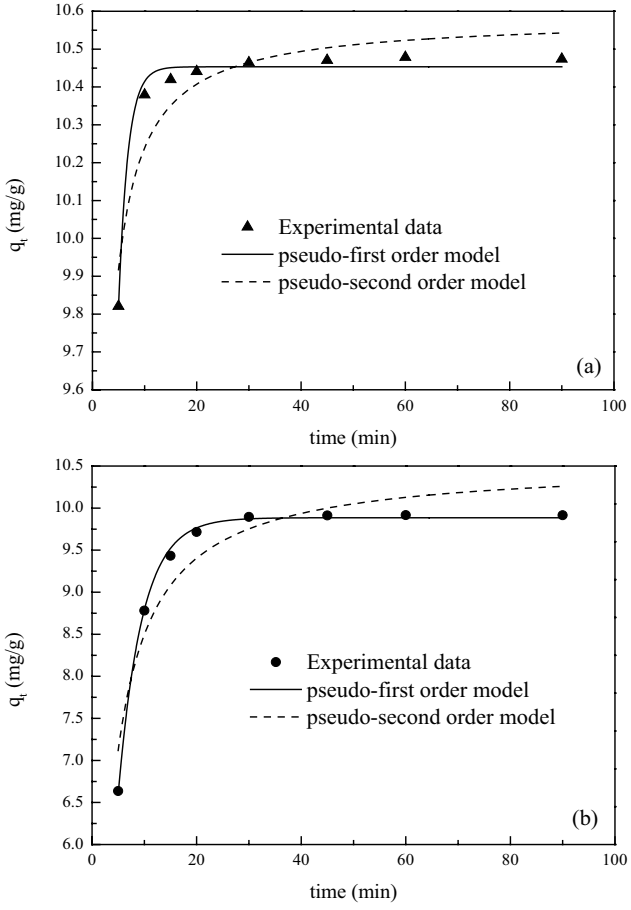

Fig. S1. Fitting of kinetics for (a) Mg-Al-Cl LDHs and (b) Mg-Al-NO_3 LDHs.